European Journal of Applied Sciences – Vol. 11, No. 1
Publication Date: January 25, 2023
DOI:10.14738/aivp.111.13776.
Meurant, R. C. (2023). The Morphology of the Regular & Semi-Regular Polyhedra and Tessellations According to the Separation of Facial Polytopes. European Journal of Applied Sciences, 11(1). 147–167.

The morphology of the regular & semi-regular polyhedra and tessellations according to the separation of facial polytopes

Robert C. Meurant
Director Emeritus, Institute of Traditional Studies;
Adjunct Professor, Seoul National University PG College of Eng.;
Exec. Director, Research & Education, Harrisco Enco
4/1108 Shin-Seung Apt, ShinGok-Dong 685 Bungi,
Uijeongbu-Si, Gyeonggi-Do 11741, Republic of Korea.
rmeurant@gmail.com • http://www.rmeurant.com/its/

ABSTRACT

In previous work, inspired by Critchlow [1], and by Grünbaum & Shephard [2], I proposed an integral 2.5D cubic schema of the regular and semi-regular polyhedra and polygonal tessellations of the plane for each class of symmetry, which could be differentiated into an upper and lower layer of 4 polytopes each, and characterized by corresponding pairs, so that upper polytope always corresponds to lower [3]. I explored the motif of paired two-step sequences of first alternating facial separation and morphological transformation, and second facial morphological transformation and separation, which in the 2D consideration of the 2.5D schema are disposed about the vertical axis, as characterized by the correspondence between the *PPs* of the lower and upper squares (diamonds or rhombi).

Following sustained research [3−11], I here focus on a deeper pattern of morphological transformation of the primary prototypes that is characterized by the separation of one gendered set of the negative (–ve), neutral (ntrl), or positive (+ve) facial polytopes along the Y, Z, & X axes of the cubic schema. As one set of faces separates, the other two sets morph/ project if polar/neutral, through null→regular or quasi-regular→double facial levels (0→α|β→2) of the rhombic schema or its reflection. Each facial set separates just once: d=0→1. The cubic schema reveals significant three-fold symmetry by gender. The separation of faces provides an adequate schema for the morphology of the three classes of the regular and semi-regular polyhedra of {2,3,3}, {2,3,4}, and {2,3,5} symmetry, and two classes of polygonal tessellations (tilings) of {2,3,6} and {2,4,4} symmetry. (Kindly refer to Nomenclature at the end of paper).

Key words: polyhedra, tessellations, morphology, separation of faces

1. PAIRING OF POLYHEDRA BY THE SEPARATION OF FACES: CLASS II & GENERIC

The pairings of polyhedra within any one class can be characterized by the separation of one set of the negative, neutral, or positive surface polytopes on the Y, Z, or X axes, respectively, of the 2.5D schema, as in Fig. 1. Therefore, three significant kinds of pairings of *PP*s can be made in the 2.5D schema, dependent on the schema orthogonal axis. For descriptive convenience, this is described for Class II of {2,3,4} symmetry, where the −ve, neutral, and +ve axes of the class, and thus of each of its individual polytopes, are conveniently the √1, √2, and √3 (100, 110, 111) axes of the cube, respectively.

This class is of 3D polyhedra, and the +ve and −ve polar polytopes take different forms (unlike Class I of 3D polyhedra, where the polar polytopes take the same form of the tetrahedron, though in alternative orientation, or Class V of 2D polygons, where both polar polytopes also take the same form of the square, but in different location). In the other classes, the symmetry axes are not in general orthogonal; in addition, Class II (leaving aside the transitional Snub form) precisely constitutes the *PP*s of the Class III honeycombs, so are the primary components of the Class III honeycomb periodic all-space-filling arrays. Subsequently, I compare this Class II with Class IV, to illustrate the differences between 3D polyhedral and 2D polygonal form, while considering classes with different polar polytopes, as opposed to having the same, but reoriented (3D) or relocated (2D) form. Contemplation of Fig. 1 reveals the beautiful integrity of interrelationship:

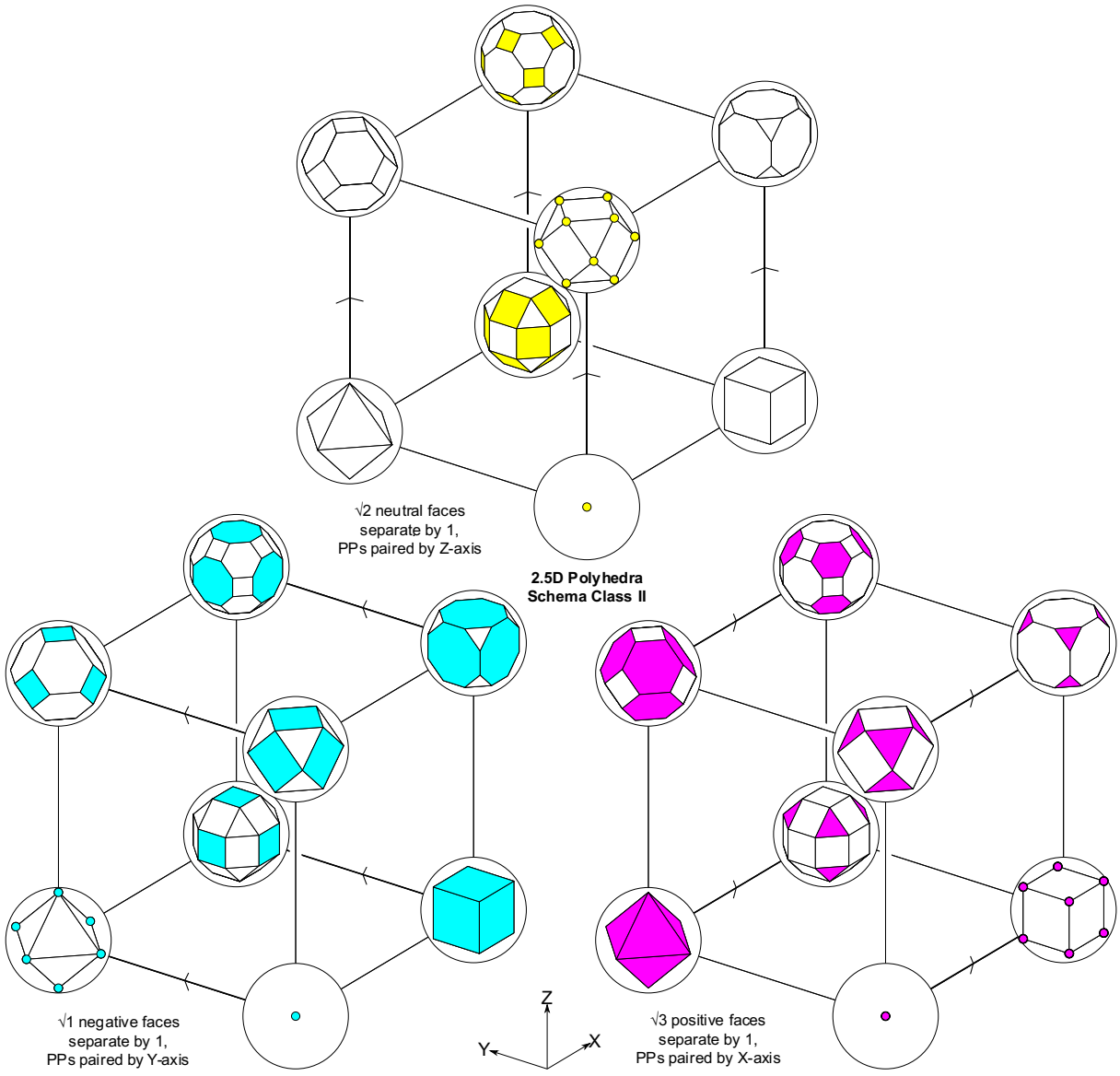

Fig. 1: Pairings of the Class II polyhedra according to −ve (left), ntrl (upper), or +ve (right) faces, which separate from adjoining (sharing a *V* or *E*) to adjacent by distance unit 1 = edge length. *CB* and *OH* are considered the −ve and +ve polar polytopes, respectively, with facial *PT*s shown as −ve (cyan) & +ve (magenta), respectively, with ntrl polytopes are shown in yellow, or thick black edge.

Table I. Separating *PP* pairs for Class II and their source and goal polytopes.

Negative			Neutral			Positive		
Separating facial *PT*s	Source polytope	Goal polytope	Separating facial *PT*s	Source polytope	Goal polytope	Separating facial *PT*s	Source polytope	Goal polytope
V^-	VP_2	OH	V^0	VP_2	CO	V^+	VP_2	CB
SQ^-	CB	$SRCO$	E^0_α	OH	TO	TR^+	OH	$SRCO$
RS^-	CO	TO	E^0_β	CB	TC	RT^+	CO	TC
OG^-	TC	$GRCO$	SQ^0	$SRCO$	$GRCO$	HX^+	TO	$GRCO$

NB. In this paper, I modify my previous conventions, so Vertex $VT \rightarrow V$; neutral vertex $NV \rightarrow V^0$; edge $EG \rightarrow E$, neutral edge $NE \rightarrow E^0$; neutral square $NS \rightarrow SQ^0$; Facial polytope → F; on-axis 0D V^0 (the 1-gon, of 1 E & 1 V^0) & 1D E^0 (the 2-gon, of 2 E & 2 V^0), & 2D polygons (TR, HX, SQ, …), are considered F; see Nomenclature at end.

On the Y-axis of the schema (going leftwards), *negative* faces separate (cyan; lower left). Adjoining (coincident) V^-s of the VP separate to adjacent V^-s of the OH (its nodes); adjoining SQ^-s of the CB separate to adjacent SQ^-s of the $SRCO$; adjoining RS^-s of the CO separate to adjacent RS^-s of the TO; and adjoining OG^-s of the TC separate to adjacent OG^-s of the $GRCO$. In each case, *adjoining* pairs of negative polytopes of a PP that share a V^0 or E^0 separate by edge length unit distance 1 to *adjacent* negative polytopes of its PP pair.

On the Z-axis of the schema (going upwards), *neutral* faces separate (yellow; upper). Adjoining (coincident) V^0s of the VP separate to adjacent V^0s of the CO (its nodes); adjoining E^0s of the OH separate to adjacent E^0s of the TO; adjoining E^0s of the CB separate to adjacent E^0s of the TC; and adjoining SQ^0s of the $SRCO$ separate to adjacent SQ^0s of the $GRCO$. In each case, adjoining pairs of neutral surface polytopes of a PP, sharing a V or E that need not be +/0/−ve, e.g., of $SRCO$, separate by d=1 to adjacent neutral Fs of its PP pair.

On the X-axis of the schema (going rightwards), *positive* faces separate (magenta; lower right). Adjoining (coincident) V^+s of the VP separate to adjacent V^+s of the CB (its nodes); adjoining TR^+s of the OH separate to adjacent TR^+s of the $SRCO$; adjoining RT^+s of the CO separate to adjacent RT^+s of the TC; & adjoining HX^+s of the TO separate to adjacent HX^+s of the $GRCO$. In each case, adjoining pairs of positive polytopes of a PP sharing V^0 or E^0 separate by d = 1 to adjacent +ve polytopes of its PP pair.

These various correspondences by separation of facial polytopes by unit distance can be combined into the one illustration (Fig. 2), shown at left & middle for Class II, and at right for all classes. Again, in each case of facial separation, *adjoining* pairs of polytopes of a PP (d=0) separate by unit distance d=1 (= length of polytope side) to *adjacent* polytopes of its PP pair:

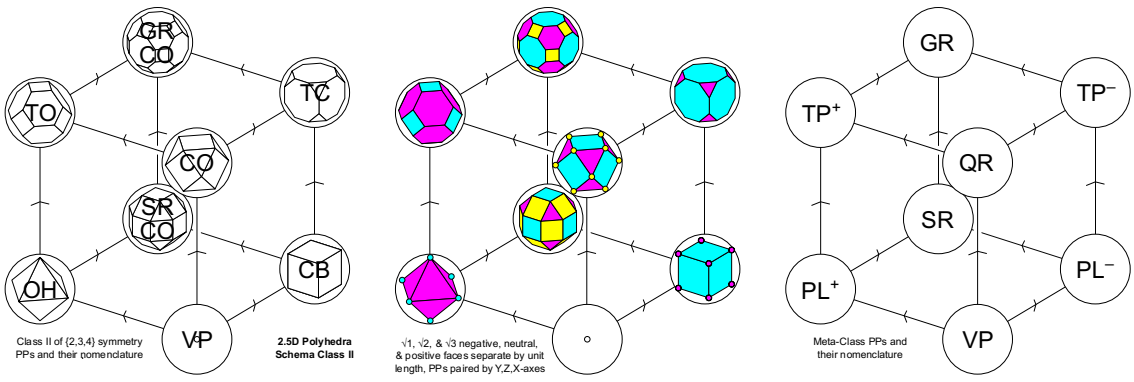

Fig. 2: Paired correspondences of *PP*s for Class II (left & middle), & generically (all classes; right).

2. THE ASSOCIATED EVOLUTION OF NON-SEPARATING MORPHING FACES: CLASS II

As partially explored in earlier papers [3, 4] and further to the description in the previous section, as one set of faces separates, the other 2 sets of faces evolve. Refer Fig. 3 & Table III.

In Class II, the neutral polytopes α & β of level 1 ($L1$) are the edges of the +ve OH & −ve CB, and the corresponding edges of the +ve TO & TC, respectively. α & β complement one another:

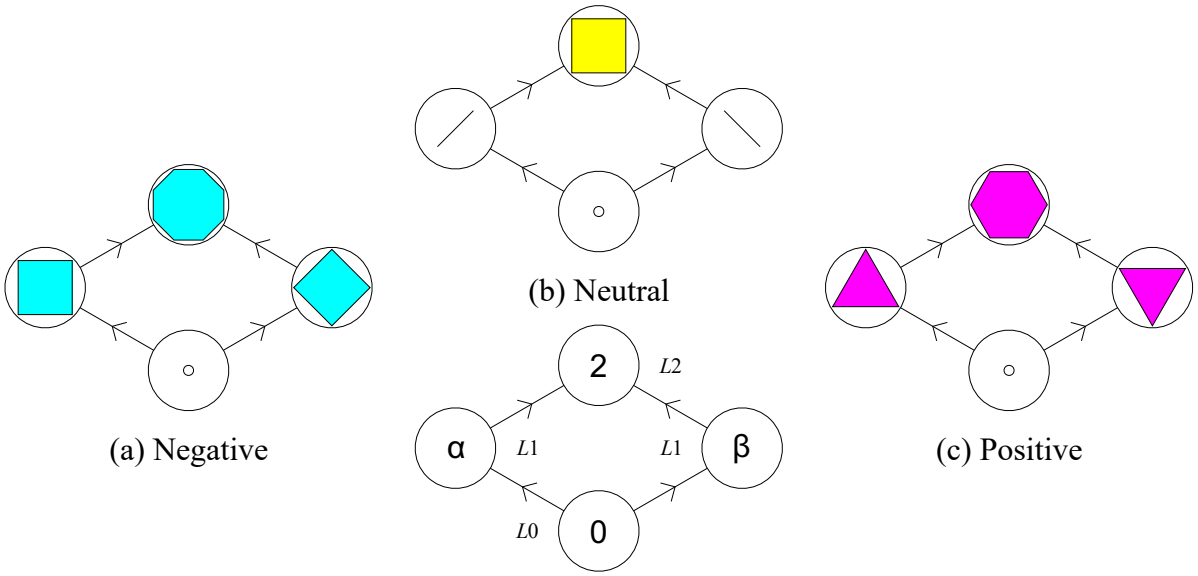

Fig. 3: Rhombic schema of the levels of development of the polar facial polytopes:
(a)–(c) Class II –ve, ntrl, & +ve facial polytopes; (d) Generic schema of all Classes I–V.

Negative Separations: On the Y-axis of the cubic schema going leftwards, as the −ve faces (cyan) separate, the +ve faces expand, evolving according to the rhombic schema of Fig. 3c from one level to the next higher level. Simultaneously, the neutral faces project (extrude), evolving to an analogous rhombic schema from one level to the next higher level (Fig. 3b). In Class II, as (lower rhomb) V^-s & SQ^-s separate, V^+s expand to TR^+s; while (upper rhomb) as RS^-s and OG^-s separate, RT^+s expand to HX^+s; and meanwhile, (lower & upper rhombs) V^0s and E_βs project to E_αs and SQ^0s, respectively (Fig. 1, lower left).

Neutral Separations: On the Z-axis of the cubic schema going upwards, as the neutral faces separate, both the +ve and the −ve faces expand, evolving according to the rhombic schema from one level to the next higher level (Fig. 3d). In Class II, as (front right rhomb) V^0s and E^0_βs separate, V^+s morph to RT^+s; and as (back left rhomb) E^0_αs and SQ^0s separate, TR^+s morph to HX^+s. As (front left rhomb) V^0s & E^0_αs separate, V^-s morph to RS^-s; and as (back right rhomb) E^0_βs & SQ^0s separate, SQ^-s morph to OG^-s (Fig. 1, upper middle).

Positive Separations: On the X-axis of the schema going rightwards, as the +ve faces separate, the −ve faces expand, evolving according to the rhombic schema from one level to the next higher level (Fig. 3a). Meanwhile, the neutral faces project (extrude), evolving according to the analogous rhombic schema from one level to the next higher level (Fig. 3b). In Class II, as (lower rhomb) V^+s & TR^+s separate, V^-s expand to SQ^-s; while (upper rhomb) as RT^+s and HX^+s separate, RS^-s expand to OG^-s; meanwhile, (lower & upper rhombs) V^0s and E^0_αs extrude to E^0_βs and SQ^0s, respectively (Fig. 1, lower right).

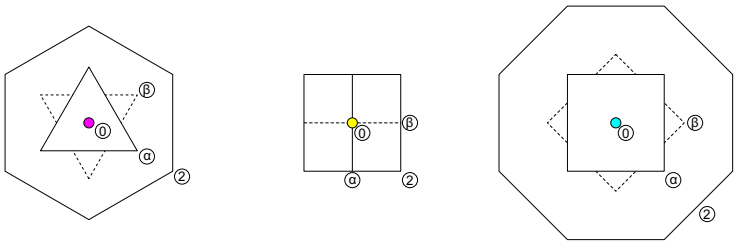

Fig. 4: On-axis Class II null, regular/quasi-regular (dashed), & double (frequency) (0, α & β, 2) faces from center VT (circle) outwards and front to back for (left to right): +ve, ntrl, and −ve axes; null (0) refers to the 0D case; regular (α) to the same orientation face as for the regular PLs (OH, CB), and quasi-regular (β) as for the quasi-regular QR (CO); and double (2) to the 2-frequency face. Neutral α & β faces are defined as the 2-gon E^0s of the +ve & −ve PLs OH & CB, respectively.

The neutral faces (2-gon neutral edges of the PP) that are generated at the middle Level 1 $L1$) of the facial rhombic schema shown in Fig. 3 are of two kinds of orientations, α & β, depending on whether they characterize the +ve or −ve PLs (in Class II, OH & CB), respectively. This is similar to the central $L1$ distinction of the +ve and −ve faces into α | β orientations (Figs. 3b & 4). The morphology of the α|β neutral dichotomy is analogous to that of the two kinds of neutral polyhedra of the Class III honeycombs, especially in the primary and tertiary arrays [5−11], where the neutral diverges into complementary pairs.

Table II. Generic Schema of the 5 Classes of the Regular & Semi-regular Polyhedra & Tilings.

Polytope	Symmetry	Lower Rhomb				Upper Rhomb			
Class	{0,+,−}	VP	P^+	P^-	SR	QR	$TrncP^+$	$TrncP^-$	GR
I	{2,3,3}	VP_I	TH^+	TH^-	$SR\ TH{:}TH$	$TH{:}TH$	TT^+	TT^-	$GR\ TH{:}TH$
II	{2,3,4}	VP_{II}	OH^+	CB^-	$SR\ OH{:}CB$	$OH{:}CB$	TO^+	TC^-	$GR\ OH{:}CB$
III	{2,3,5}	VP_{III}	IC^+	DC^-	$SR\ IC{:}DC$	$IC{:}DC$	TI^+	TD^-	$GR\ IC{:}DC$
IV	{2,3,6}	VP_{IV}	TR^+	HX^-	$SR\ TR{:}HX$	$TR{:}HX$	RT^+	RH^-	$GR\ TR{:}HX$
V	{2,4,4}	VP_V	SQ^+	SQ^-	$SR\ SQ{:}SQ$	$SQ{:}SQ$	RS^+	SQ^-	$GR\ SQ{:}SQ$

Table III. Class II Separation of one set of (−ve, ntrl, or +ve) facial pairs of PPs with associated morphological changes of the other two sets of facial polytopes from source to goal ($OH{:}\,CB{=}CO$).

Separating facial PTs	Primary Polytope (PP) transition	Source facial PTs	Goal facial PTs	Source facial PTs	Goal facial PTs
Negative facial PT separation		Neutral facial PT projection		Positive facial PT expansion	
V^-	$VP_2 \rightarrow OH$	${}_0V^0$	${}_0E^0_\alpha$	${}_0V^+$	${}_0TR^+$
SQ^-	$CB \rightarrow SRCO$	${}_0E^0_\beta$	${}_0SQ^0$	${}_1V^+$	${}_1TR^+$
RS^-	$CO \rightarrow TO$	${}_1V^0$	${}_1E^0_\alpha$	${}_0RT^+$	${}_0HX^+$
OG^-	$TC \rightarrow GRCO$	${}_1E^0_\beta$	${}_1SQ^0$	${}_1RT^+$	${}_1HX^+$
Neutral facial PT separation		Positive facial PT expansion		Negative facial PT expansion	
V^0	$VP_2 \rightarrow CO$	${}_0V^+$	${}_0RT^+$	${}_0V^-$	${}_0RS^-$
E^0_α	$OH \rightarrow TO$	${}_0TR^+$	${}_0HX^+$	${}_1V^-$	${}_1RS^-$
E^0_β	$CB \rightarrow TC$	${}_1V^+$	${}_1RT^+$	${}_0SQ^-$	${}_0OG^-$
SQ^0	$SRCO \rightarrow GRCO$	${}_1TR^+$	${}_1HX^+$	${}_1SQ^-$	${}_1OG^-$
Positive facial PT separation		Negative facial PT expansion		Neutral facial PT projection	
V^+	$VP_2 \rightarrow CB$	${}_0V^-$	${}_0SQ^-$	${}_0V^0$	${}_0E^0_\beta$
TR^+	$OH \rightarrow SRCO$	${}_1V^-$	${}_1SQ^-$	${}_0E^0_\alpha$	${}_0SQ^0$
RT^+	$CO \rightarrow TC$	${}_0RS^-$	${}_0OG^-$	${}_1V^0$	${}_1E^0_\beta$
HX^+	$TO \rightarrow GRCO$	${}_1RS^-$	${}_1OG^-$	${}_1E^0_\alpha$	${}_1SQ^0$

3. PAIRING OF POLYGONAL ARRAYS BY THE SEPARATION OF FACES: CLASS IV

Class IV of the regular and semiregular polytopes comprises the *Tri−Hex* arrays, where the polar polytopes are the +ve triangular and −ve hexagonal regular tessellations. A similar characterization to that made for Class II applies to Class IV, notwithstanding that it significantly differs, being of 2D tessellations, rather than 3D polyhedra, and unlike the other 2D Class V of the $SQ{-}SQ$ cluster of arrays, has polar elements of different geometric form.

Negative Separations: On the Y-axis of the cubic schema going leftwards, as (lower rhomb) V^-s & HX^-s separate, V^+s expand to TR^+s; while (upper rhomb) as RH^-s and DD^-s separate, RT^+s expand to HX^+s; and meanwhile, (lower & upper rhombs) V^0s and E_βs project to E_αs and SQ^0s, respectively (Fig. 5, left).

Neutral Separations: On the Z-axis of the cubic schema going upwards, as (front right rhomb) V^0s and E_β^0s separate, V^+s morph to RT^+s; as (back left rhomb) E_α^0s and SQ^0s separate, TR^+s morph to HX^+s. As (front left rhomb) V^0s & E_α^0s separate, V^-s morph to RH^-s; and as (upper right rhomb) E_β^0s & SQ^0s separate, HX^-s morph to DD^-s (Fig. 5, top).

Positive Separations: On the X-axis of the cubic schema going rightwards, as (lower rhomb) V^+s & TR^+s separate, V^-s expand to HX^-s; while (upper rhomb) as RT^+s and HX^+s separate, RH^-s expand to DD^-s; meanwhile, (lower & upper rhombs) V^0s and E_α^0s extrude to E_βs and SQ^0s, respectively (Fig. 5, right).

Figure 5 on this page and the next show for each cluster:

UPPER RHOMBUS:
Great Rhombic Tri−Hex Array (top);
Truncated Triangular Array | Truncated Hexagonal Array (upper left | right);
Quasi-Regular TriHex array (lower).

LOWER RHOMBUS:
Small Rhombic Tri−Hex array (upper);
Triangular Array | Hexagonal Array (lower left | right);
Verticial Array (bottom).

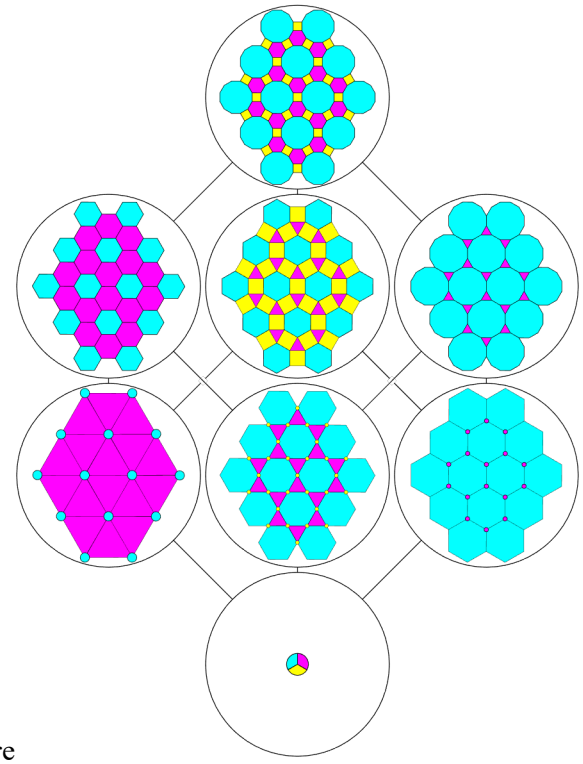

In this class, the hexagonal and triangular arrays are considered the −ve & +ve polar polytopes, respectively, their facial axes being the −ve (light grey) and +ve (dark grey) axes.

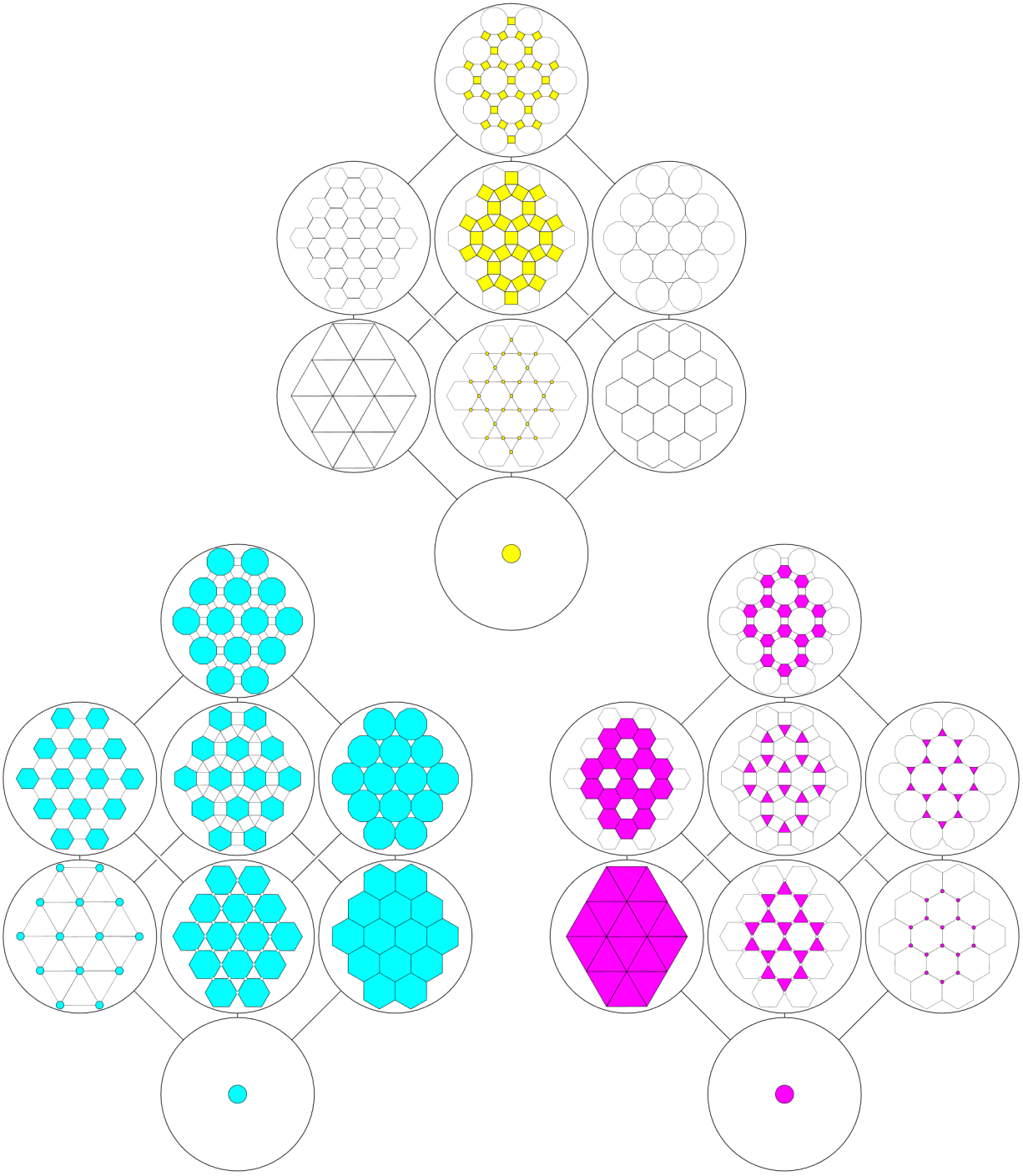

Fig. 5: 2.5D Schema of faces: Pairing of the Class IV polyhedra according to their −ve (lower left), ntrl (upper left), and +ve (lower right), faces; with (previous page) their combined positive, neutral, and negative faces.

4. THE UNFOLDING OF APPARENT THREE-FOLD SYMMETRY

I had previously [3] exploited the 2D characteristics of the 2.5D schema, integrating the vertical dimension, and associated separation of PP elements into +ve (left; $OH-TO$), neutral (middle; $VP–CO–SRCO–GRCO$), and −ve (right; $CB–TC$). The 3D characteristics of the schema were partially employed, with primary differentiation into lower (VP, OH, CB, $SRCO$) and upper (CO, TO, TC, $GRCO$) rhombi (top & bottom faces of the cubic schema). Generically, this represents separation into positive $TP^{+}–PL^{+}$, neutral $VP–QR–SR–GR$, and negative $PL^{-}–TP^{-}$, with lower (VP, PL^{+}, PL^{-}, SR) and upper (QR, TP^{+}, TP^{-}, GR) rhombi.

In this paper, these 3D characteristics are more fully developed by regarding the √3 long diagonal VP—$GRCO$ as the primary axis, and situated vertically, so the cubic schema can be regarded as a cube balanced on one vertex (VP) (Fig. 6b), hence demonstrating 3-fold symmetry: instead of considering +ve and −ve as polar opposites with neutral as central mediating case, the three gender cases of +ve, neutral, and −ve are allowed a measure of equal status, the main distinction being that the neutral faces (2-gon neutral edges of the PP) that are generated at Level 1 of the facial hierarchy are of two orientations, α & β, as before.

Considering the cubic schema in a true 3D multi-axial sense (in microgravity), it is evident that any PP enjoys various kinds of pairing relationship with 3 adjoining PPs, 3 distant PPs, and 1 opposite PP; e.g. in Class II, OH—TC: OH; SR, VP, TO; CO, GR, CB; TC. On the primary VP—$GRCO$ √3 axis, the VP shows a stepped progression through 3 neighboring PPs, OH, CO, CB; 3 more distant relatives, TC, $SRCO$, TO; to culminate in its opposite, $GRCO$.

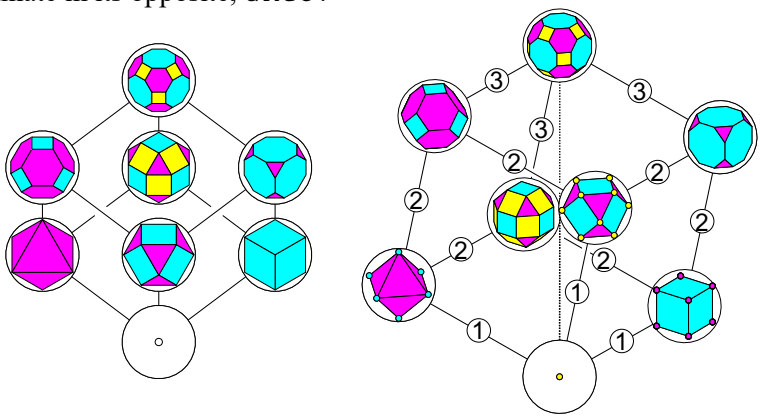

Fig. 6: (left) Class II rhombic bi-hierarchical network of PPs (view +ve axis); (right) Class II VP—$GRCO$ √3 axis with stepped progression of PP pairs of VP to 1: $OH/CO/CB$; to 2: $TC/SRCO/TO$; to 3. $GRCO$.

Therefore, regarding the $GRCO$—VP diagonal as a unique vertical primary axis to the schema (restoring gravity), each of the PPs can be regarded as a locus of realization and/or of generation of its neighboring PPs, and the 8 PPs of each class can then be ranked according to their pattern of relationship to their adjoining PPs: VP is unique, and in step 1, generates 3 equivalent PPs: $VP \rightarrow OH$, CO, & CB. In step 2, OH, CO, & CB each generate two PPs, i.e., $OH \rightarrow SRCO$ & TO; $CO \rightarrow TO$ & TC; and $CB \rightarrow TC$ & $SRCO$. In step 3, the equivalent TC, $SRCO$, & TO each generate the unique $GRCO$: TC, $SRCO$, & $TO \rightarrow GRCO$, to culminate the vertical progression. The constant feature of each step instance is the separation of faces of one gender (−, 0, +) by unit distance, to indicate that this may be the driving characteristic.

Hence the schema displays clear stratification (as for the cubic polar zonahedron [12]), with each PP being generated from, and/or developing into, its fellow PPs (where VT only generates; $GRCO$ is only generated), there being 4 strata (S) of elements: $S1$: VP; $S2$: OH, CO, & CB; $S3$: TC, $SRCO$, & TO; and

$S4$: $GRCO$. The schema's morphology exhibits clear 3-fold order around the VP—$GRCO$ √3 axis; each of the 5 Classes I–V of regular & semi-regular polytopes according to symmetry is characterized by a development sheath of sequences from VP to GR of 3-fold nature, with the PPs of a class disposed at those 4 strata.

Then for each of the five classes, each constituent PP within that class can be developed by the separation of −ve, neutral, or +ve faces from the source VP in a sequence of steps, so: 0 step: VP; 1 step: PL^+, QR, PL^-; 2 steps: TP^-, $SRQR$, TP^+; 3 steps: $GRQR$ (Fig. 7b). The variations in steps to realize a PP by the separation of adjoining surface polytopes separating by unit distance to adjacent surface polytopes can be given as: no way: VP; one way: PL^+, QR, PL^-; two ways: TP^-, $SRQR$, TP^+; and six ways: $GRQR$.

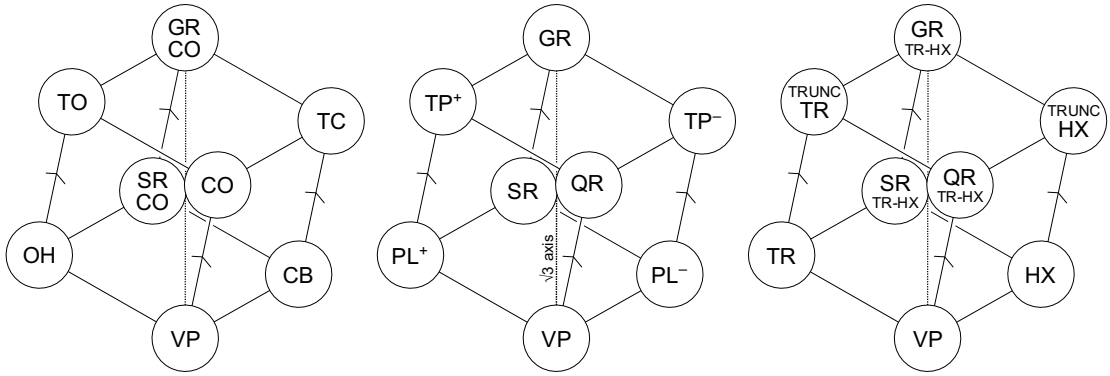

Fig. 7: The 3-fold order and pairing of polytopes by neutral faces and their separation: (a) Class II, (b) Generic, i.e., for all 5 classes of symmetry, (c) Class IV.

For Class II, this is 0 step (variations in steps of no way), VP_{II}; 1 step (1 way), OH, CO, CB; 2 steps (2 ways), TC, $SRCO$, TO; 3 steps (6 ways), $GRCO$ (Fig. 7a). For Class IV, this is 0 steps (no way), VP_{IV}; 1 step (1 way), TR, $QR\ TR{:}\,HX$, HX; 2 steps (2 ways), $TrncHX$, $SR\ TR{:}\,HX$, $TrncTR$; 3 steps (6 ways), $GR\ TR{:}\,HX$ (Fig. 7c). (*NB.* Or, subduction sequences of facial convergence could consider $GRQR \rightarrow (TP^+, SRQR, TP^-) \rightarrow (PL^+, QR, PL^-) \rightarrow VP$). Therefore, each family of polytopes demonstrates a high degree of order, and should not be thought of as being in any sense accidentally related; or within any one class, by assuming one PP is equivalent to the other seven. Rather, they simultaneously crystallize into formal existence as regularly varied concretizations of an integral, profound natural spatial order.

The 3-fold morphology of the 8 PPs in each class shows the structure of a polar zonahedron, as also observed in the evolution/involution of the 2D polar zonagon. This geometry at higher frequency (f = (12, 24, 48, 60…) is used in Islamic sacred architecture of the dome, in the 3D form and in 2D surface decoration, as explored in part of my PhD [12:pp.9−34], and offers facile advantages to construction and decoration (equal subdivision of angle in plan; equal length edges; constant vertical gain of edges; corresponding equal vertical stratification of nodes; nodes lying on rotated sine wave surface). In sacred and traditional architecture, the form can eloquently symbolize the geometry of the center, projected into time and space; the cycle of manifestation and transformation of a central epiphany emanating from the source, extending to maximum realization in the phenomenal; then reflecting, clarifying, and centering, for the manifestation to be reabsorbed through the center, to return to the noumenal beyond creation.

But the 3-fold symmetry of −ve, ntrl, and +ve is imperfect; consideration of the duality of the polyhedra indicates that the function of the neutral is different from that of the polar; there is a creative tension between this characterization and the unfolding of order from wrapping around a central axis, to reflective symmetry about a central vertical axis of neutrality; the sheath of the schema splits open to uncurl to dispose elements and relationships into bilateral symmetry of vertical qualitative differentiation, and horizontal duality/polarity. Hence the subtlety of the 2.5D schema that can mediate that creative tension.

Table IV. Generic separation of one set of (−ve, neutral, or +ve) facial pairs of PPs together with associated morphological changes of the other 2 sets of facial polytopes (Fs) from source to goal.

Separating facial PTs	Primary Polytope (PP) transition	Source facial PTs	Goal facial PTs	Source facial PTs	Goal facial PTs
Negative facial PT separation		Neutral facial PT projection		Positive facial PT expansion	
F_0^-	$VP \rightarrow PL^+$	${}_0V_0^0$	${}_0E_\alpha^0$	${}_0V_0^+$	${}_0F_\alpha^+$
F_α^-	$PL^- \rightarrow SRQR$	${}_0E_\beta^0$	${}_0F_2^0$	${}_1V_0^+$	${}_1F_\alpha^+$
F_β^-	$QR \rightarrow TP^+$	${}_1V_0^0$	${}_1E_\alpha^0$	${}_0F_\beta^+$	${}_0F_2^+$
F_2^-	$TP^- \rightarrow GRQR$	${}_1E_\beta^0$	${}_1F_2^0$	${}_1F_\beta^+$	${}_1F_2^+$
Neutral facial PT separation		Positive facial PT expansion		Negative facial PT expansion	
F_0^0	$VP \rightarrow QR$	${}_0V_0^+$	${}_0F_\beta^+$	${}_0V_0^-$	${}_0F_\beta^-$
F_α^0	$PL^+ \rightarrow TP^+$	${}_0F_\alpha^+$	${}_0F_2^+$	${}_1V_0^-$	${}_1F_\beta^-$
F_β^0	$PL^- \rightarrow TP^-$	${}_1V_0^+$	${}_1F_\beta^+$	${}_0F_\alpha^-$	${}_0F_2^-$
F_2^0	$SRQR \rightarrow GRQR$	${}_1F_\alpha^+$	${}_1F_2^+$	${}_1F_\alpha^-$	${}_1F_2^-$
Positive facial PT separation		Negative facial PT expansion		Neutral facial PT projection	
F_0^+	$VP \rightarrow PL^-$	${}_0V_0^-$	${}_0F_\alpha^-$	${}_0V_0^0$	${}_0E_\beta^0$
F_α^+	$PL^+ \rightarrow SRQR$	${}_1V_0^-$	${}_1F_\alpha^-$	${}_0E_\alpha^0$	${}_0F_2^0$
F_β^+	$QR \rightarrow TP^-$	${}_0F_\beta^-$	${}_0F_2^-$	${}_1V_0^0$	${}_1E_\beta^0$
F_2^+	$TP^+ \rightarrow GRQR$	${}_1F_\beta^-$	${}_1F_2^-$	${}_1E_\alpha^0$	${}_1F_2^0$

These correspondences between classes of the various facial transformations of separation, morphing/expansion of the −ve or +ve faces or extrusion/projection of the neutral faces help validate the 2.5D schema and the rhombic schema of evolution of faces, while serving to characterize the progressions and interrelationships of the polyhedra and tessellations.

In the following Figs. 8 and 9, F = Face, including where relevant (on axis) null or degenerate 0D VT and 1D E, as well as 2D polygons.

Right superscript: Polarity, of –, negative; 0, neutral; or +, positive.

Left subscript: Spacing of faces of d=0 : adjoining, or d=1 : adjacent, with 1 = edge length of polytope.

Right subscript: Hierarchical level of face: 0 = VT; α: single freq. +ve face of +ve PL PT, or neutral face (edge) of polar +ve PT; β: −ve (single freq.) face ("rotated") of QR PT, or ntrl face (E) of −ve PL PT (α & β = level 1); 2: double freq. −|+ve face of TP or GR PT or ntrl face/SQ of SR or GR PT.

Letting faces be null on-axis 0D vertices or 1D edges enables formal consistency across the PPs.
Taken together, −ve, ntrl, & +ve faces form each polyhedron or tiling of the 5 symmetry classes.

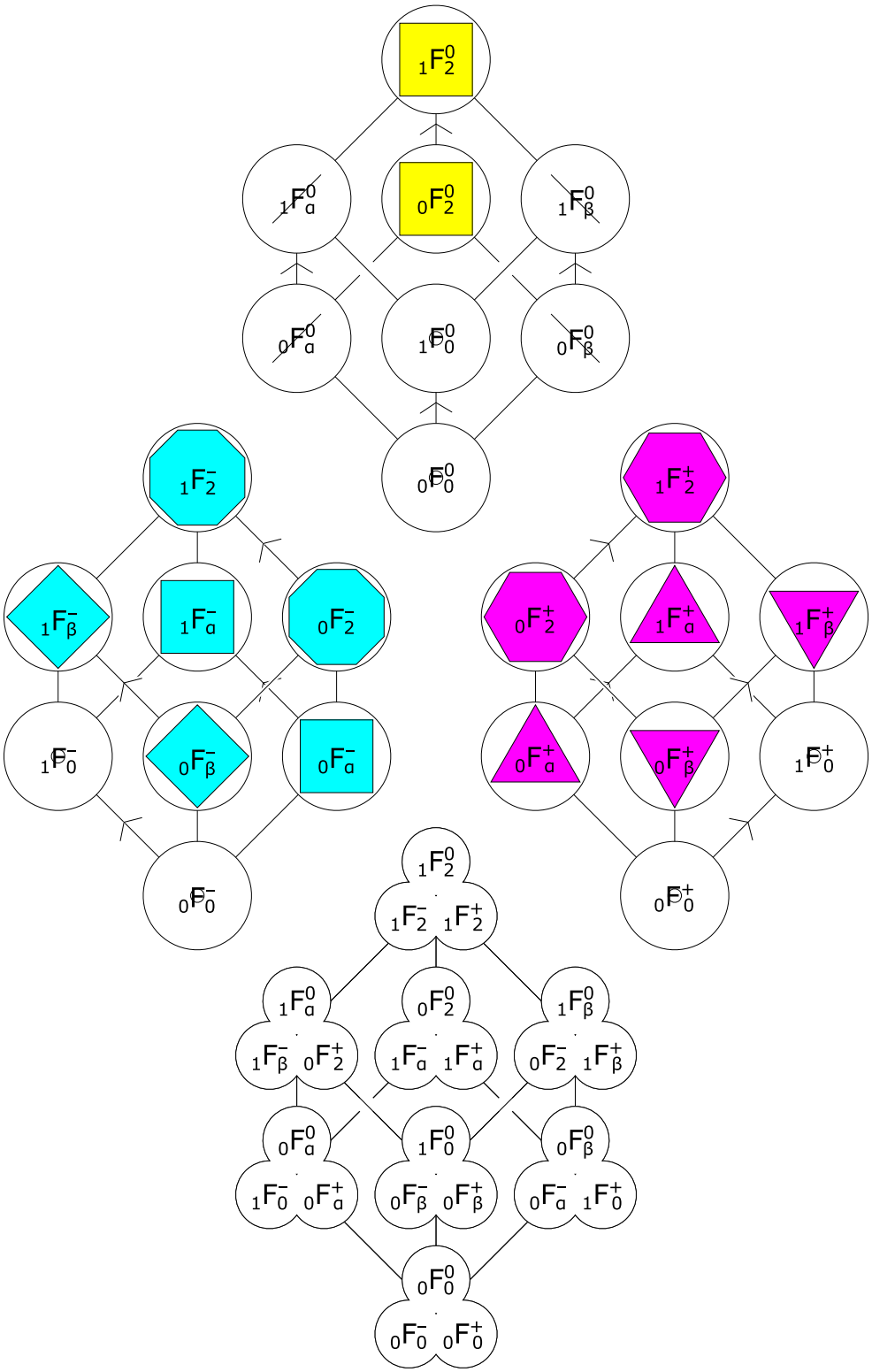

Fig. 8: Generic 2.5D Schema of faces across classes, with exemplar Class II faces: Upper: ntrl faces. Left: −ve faces. Right: +ve faces. Lower: ntrl, −ve, & +ve faces.

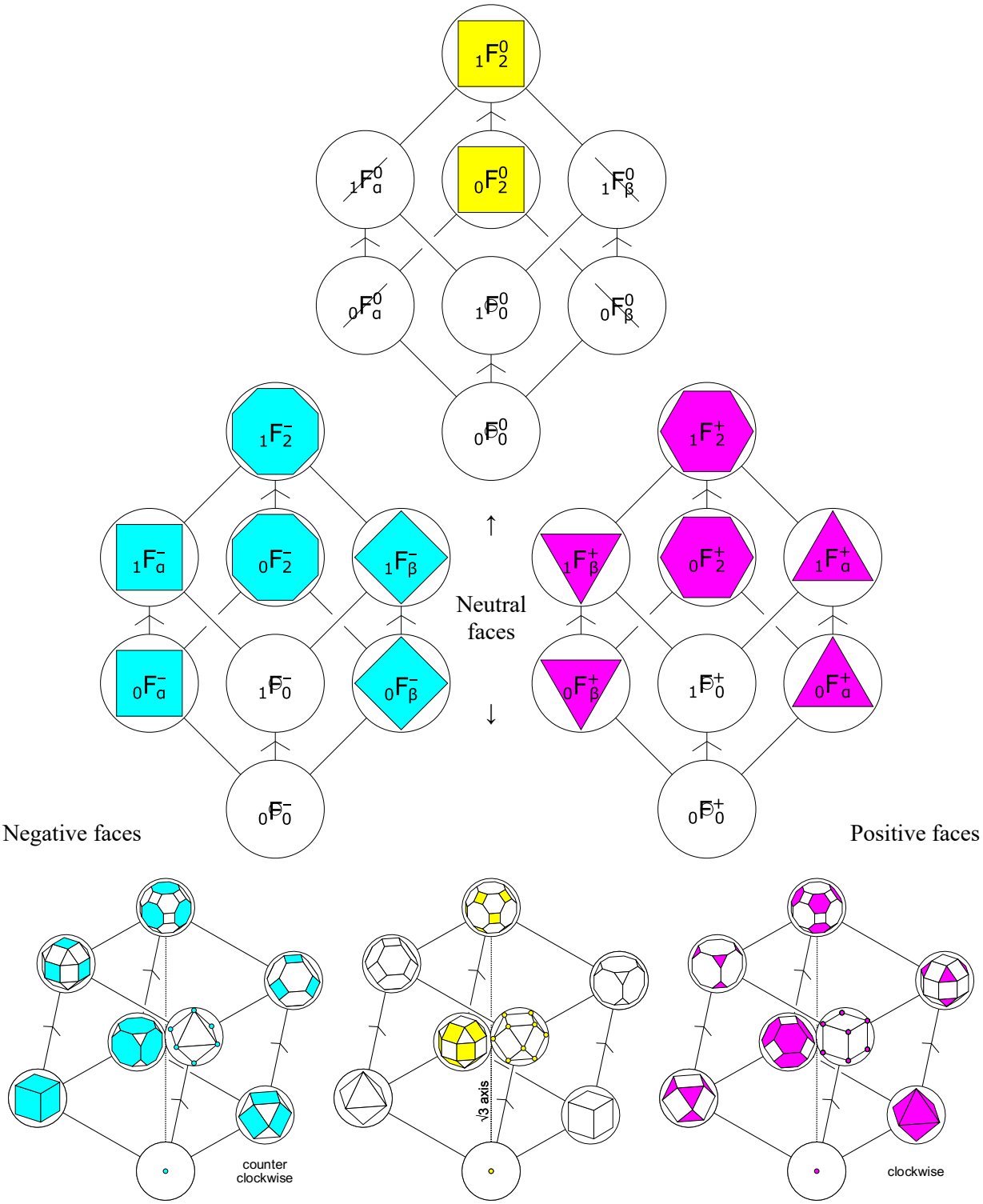

Fig. 9: Rotated Class II 2.5D Schema of faces: top/center: ntrl (0 rotation of schema); left: −ve faces (−2π/3 rotation); right: +ve faces (+2π/3). The −ve/ntrl/+ve faces combine to form each *PT*.

Faces are null; regular or quasi-regular (of the regular or quasi-regular *PT*); or double (0, α or β, or 2):

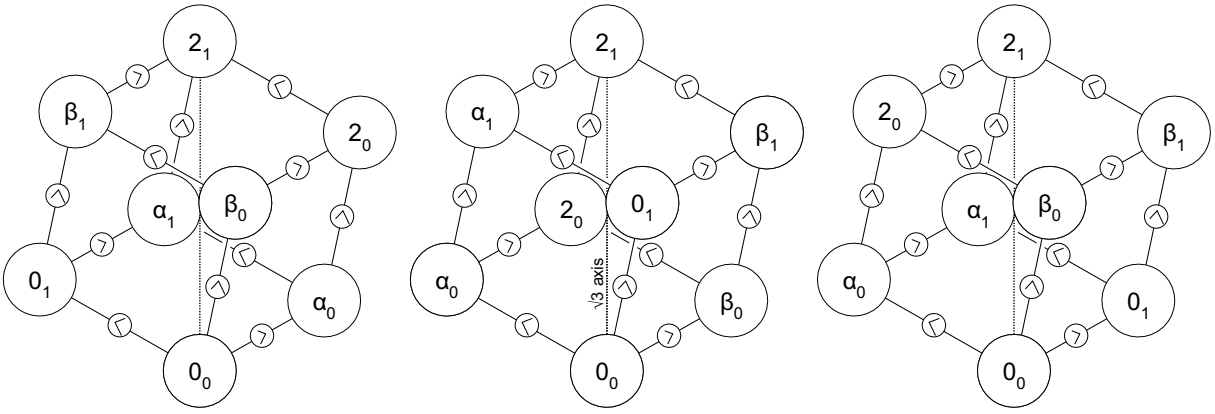

A. Negative faces
Z- & X-axes:
Front right: 0→α|β→2 rhomb d=0
Back left: 0→α|β→2 rhomb d=1
Y-axis: Separation of −ve faces
(bold) d=0 → d=1

B. Neutral faces
X- & Y-axes:
Lower: 0→α|β→2 rhomb d=0
Upper: 0→α|β→2 rhomb d=1
Z-axis: Separation of ntrl faces
(bold) d=0 → d=1

C. Positive faces
Y- & Z-axes:
Front left: 0→α|β→2 rhomb d=0
Back right: 0→α|β→2 rhomb d=1
X-axis: Separation of +ve faces
(bold) d=0 → d=1

Fig. 10: Formal patterns for left to right −ve, ntrl, & +ve clusters of faces of the cubic schema. Patterns of separation and morphing/extrusion are identical across faces, −ve & +ve reflective.

5. INTEGRATING THE RELATIONSHIPS

The formal structure of elements of the five classes of regular and semiregular polyhedra and tessellations, and the relationships between the elements in any one class, become evident. The key is the 2.5D cubic schema in concert with the rhombic schema of the development of faces, reorienting the cube on its √3 long axis of VP—GR, and recognizing the separation of faces characterizing any one of the cubic schema links between polytopes as bundles/sheaths of parallel faces of the cube as zonahedron. Then either of the other 2 sets of characteristics of the simultaneous morphing or expansion of +ve or −ve facial polytopes, and the projection or extrusion of neutral facial polytopes, can be recognized as the other 2 zonahedral bundles of the zonahedral cube, respectively, though these are not simply equivalent to the neutral case that exploits the primary orthogonal axes of the rhomb, but are differentiated into pairs of pairs that exploit the inclined axes/opposite edges of the rhomb, separating d=0 and 1 rhombs.

In the negative facial case (Fig. 10A), −ve front right cubic schema faces are adjoining d=0, while back left are adjacent d=1. On the Z-axis, the pairs of pairs are 2×(0→β) & 2×(α→2), where d=0: (0_0→β_0) & (α_0→2_0), and d=1: (0_1→β_1) & (α_1→2_1). On the X-axis, the pairs of pairs are 2×(0→α) & 2×(β→2), where d=0: (0_0→α_0) & (β_0→2_0), d=1: (0_1→α_1) & (β_1→2_1).

In the neutral facial case (Fig. 10B), neutral lower cubic schema faces are adjoining d=0, while upper are adjacent d=1. On the X-axis, the pairs of pairs are 2×(0→β) & 2×(α→2), where d=0: (0_0→β_0) & (α_0→2_0), and d=1: (0_1→β_1) & (α_1→2_1). On the Y-axis, the pairs of pairs are 2×(0→α) & 2×(β→2), where d=0: (0_0→α_0) & (β_0→2_0), d=1: (0_1→α_1) & (β_1→2_1).

In the positive facial case (Fig. 10C), +ve front left cubic schema faces are adjoining d=0, while back right are adjacent d=1. On the Y-axis, the pairs of pairs are 2×(0→α) & 2×(β→2), where d=0: (0_0→α_0) & (β_0→2_0), and d=1: (0_1→α_1) & (β_1→2_1). On the Z-axis, the pairs of pairs are 2×(0→β) & 2×(α→2), where d=0: (0_0→β_0) & (α_0→2_0), d=1: (0_1→β_1) & (α_1→2_1).

In each case of −ve, ntrl, & +ve clusters of faces, the separation of faces by gender is represented as the Y-, Z-, or X-axis separating rhombic schema of 0→α|β→2 for d=0 → d=1.

Generically, for any one class, and for each case of −ve, neutral, or +ve facial polytope, each constituent PP can be uniquely described in terms of two parameters: 1. The level of facial polytope evolution, i.e., (0, α, β, 2), and 2. the separation of facial polytope distance, whether adjoining or adjacent, i.e., (0, 1). The PPs are tabulated by F evolution & separation:

Table V. Constituent PPs of each class as generic expressions of facial evolution and separation.

Separation	Negative				Neutral				Positive			
d	0	α	β	2	0	α	β	2	0	α	β	2
0	VP	PL^-	QR	TP^-	VP	PL^+	PL^-	SR	VP	PL^+	QR	TP^+
1	PL^+	SR	TP^+	GR	QR	TP^+	TP^-	GR	PL^-	SR	TP^-	GR

Any one case: −ve, neutral, or +ve of the facial polytope, in combination with the separation (Sep.) of those neighboring facial polytopes of adjoining (d=0) or adjacent (d=1), is sufficient information to determine the PP of that class, whether VP, $PL^{-/+}$, QR/SR, $TP^{-/+}$, or GR. Excepting the QR/SR pair, the −ve and +ve cases are reflectively symmetric about the VP—GR axis, while the neutral case shows different structure, which suggests that my neutral annotation and analysis might be improved. The overall structure indicates that as well as the obvious $PL^{-/+}$ and $TP^{-/+}$ polarities, there is limited QR/SR polarity.

Generically, for any one class, and for each case of −ve, neutral, or +ve facial polytope, each constituent PP can alternatively be uniquely described according to its property of gendered −ve, neutral, and/or +ve facial separation, hence $\mathrm{d}_{-0+} = 0$ or 1:

Table VI. Constituent PPs of each class as generic expressions of facial separation d= |−0+|.

Generic			Facial separation d			Class II		
	GR			|111|			$GRCO$	
TP^+	SR	TP^-	|110|	|101|	|011|	TO	$SRCO$	TC
PL^+	QR	PL^-	|100|	|010|	|001|	OH	CO	CB
	VP			|000|			VP	

This returns the tentative 3-fold order to bilateral symmetry, and the historical perspective of the perfection of the regular PLs, though elsewhere I make an alternative case that it is the QRs that are perfect, while the PLs are extremes [13]. But given that these polyhedra and tessellations are discovered as projections of the noumenal (ideal) into the phenomenal (contingent) realm, the enigmatic possibility remains that such limited 3-fold symmetry represents a trace of primordial evolution of formal symmetry, suggests that the constraints and properties of space that we encounter might at the cosmic level be subject to change, and raises the intriguing question of whether such change would be abrupt or gradual. One might speculate whether in our cosmos, three-fold symmetry is unstable (e.g., is it common in the animal kingdom? It seems at least uncommon); and to be subsumed into a kind of 2-step bilateral symmetry that I intend to address in a subsequent paper, which is characterized by complementary forms as (−ve ↔ +ve), rather than identical, allowing the tentative self-reflective quality of the neutral ($VP \leftrightarrow GR$ and $QR \leftrightarrow SR$)). Further, can these patterns and their harmonic order be correlated with quantum forms and field behavior, where resonance seems a fundamental quality?

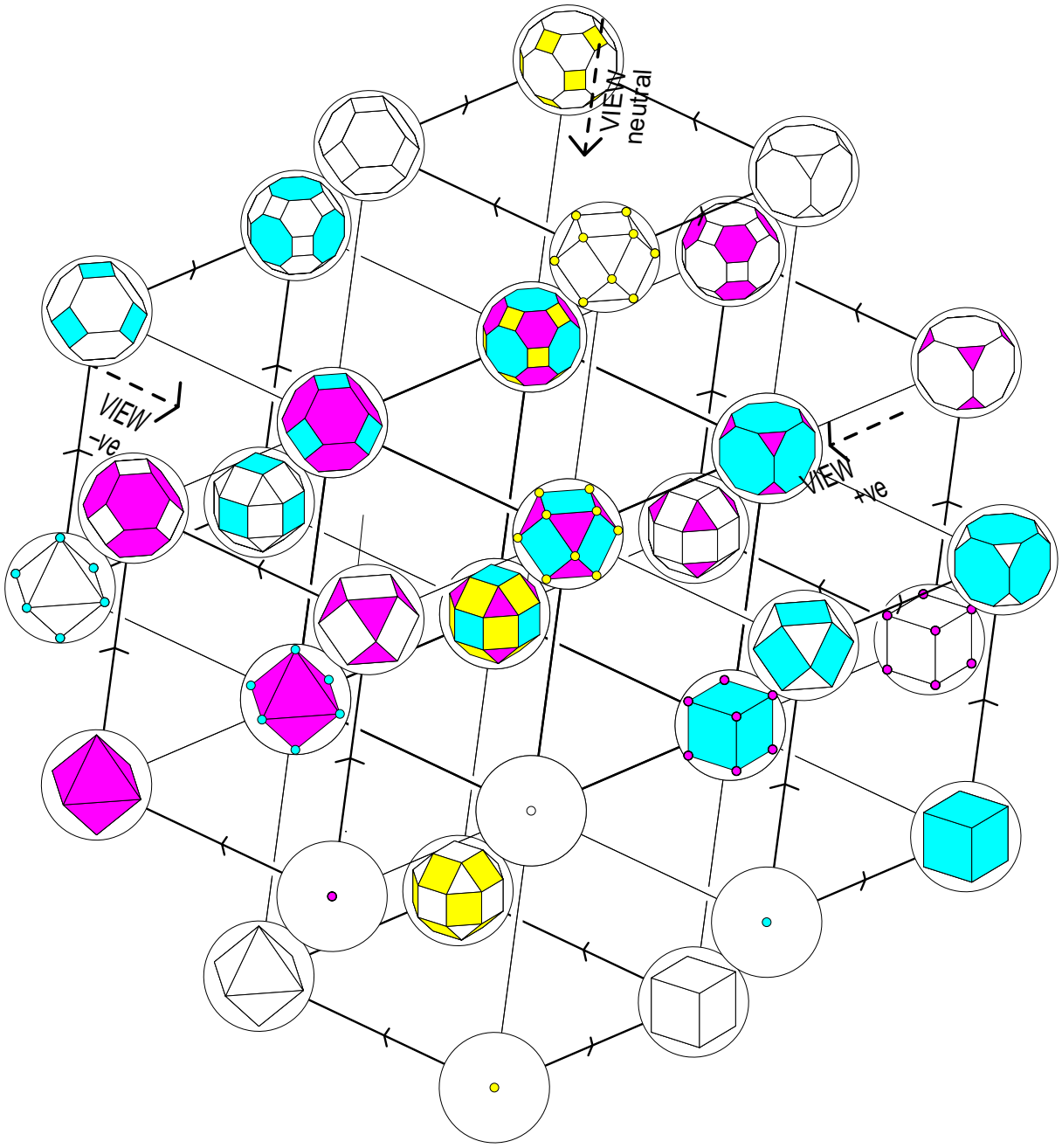

Fig. 11: Expansion of 2.5D cubic schema to demonstrate the rhombic schema on each of its six faces. Lower left, bottom, & lower right outermost faces show +ve, ntrl, and −ve (d=0) adjoining rhombic schema; upper right, top, and upper left outermost faces show +ve, ntrl, and −ve (d=1) adjacent rhombic schema.

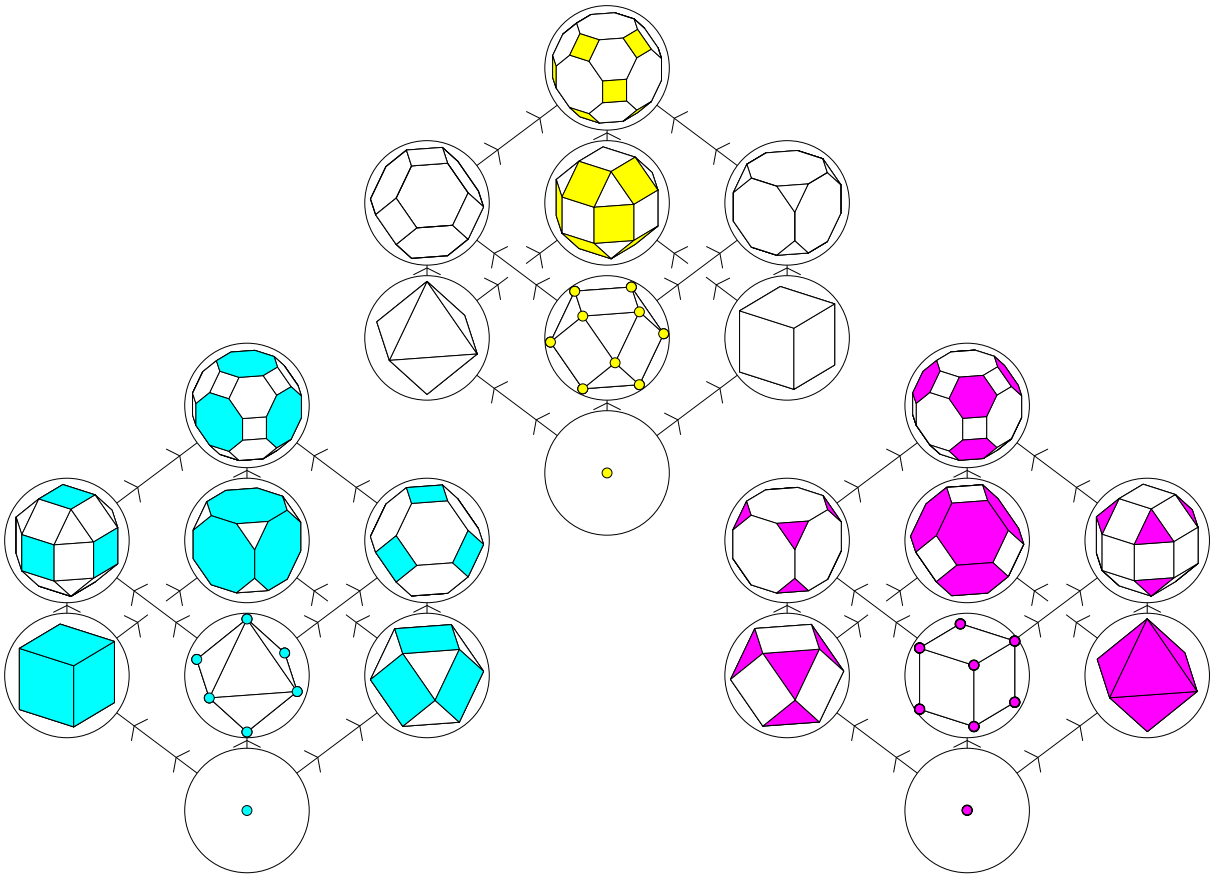

Fig. 12: Bi-rhombic (cubic) schema for the −ve (left), ntrl (center), and +ve (right) faces, abstracted from the outer 6 faces of the extended 2.5D schema in the previous figure. For consistency, 3 views are taken through the cube, one per cluster, from (outside) adjacent (d=1) to (inside) adjoining (d=0) faces.

In each cluster of Fig. 12, lower rhomb is of adjoining faces (d=0) of the polytope, upper rhomb is of the corresponding adjacent faces (d=1). Vertical links indicate these corresponding pairs. Each rotated rhomb traces the same progression of $< 0 \rightarrow \alpha|\beta \rightarrow 2 >$ of lower level 0-polytope, level 1 α & β polyhedra, and level 2 polyhedra. The −ve and ntrl clusters show α at left, while +ve shows β at left. Note the subtle "circulation" of polyhedra at the mid-levels from cluster to cluster; only the ntrl shows the initial schema, while the +ve & −ve are rotated. These clusters correspond to those of Fig. 8, so the −ve schema (cluster) is rotated counter-clockwise ($-2\pi/3$) from the ntrl schema (cluster) about the vertical GR—VP main $\sqrt{3}$ axis, while the +ve schema is rotated clockwise ($+2\pi/3$); bear in mind that in this figure, the polyhedra of the schema rotate (as a group), while their relationships (the schema edges) are conserved through the three states of −ve, ntrl, and +ve.

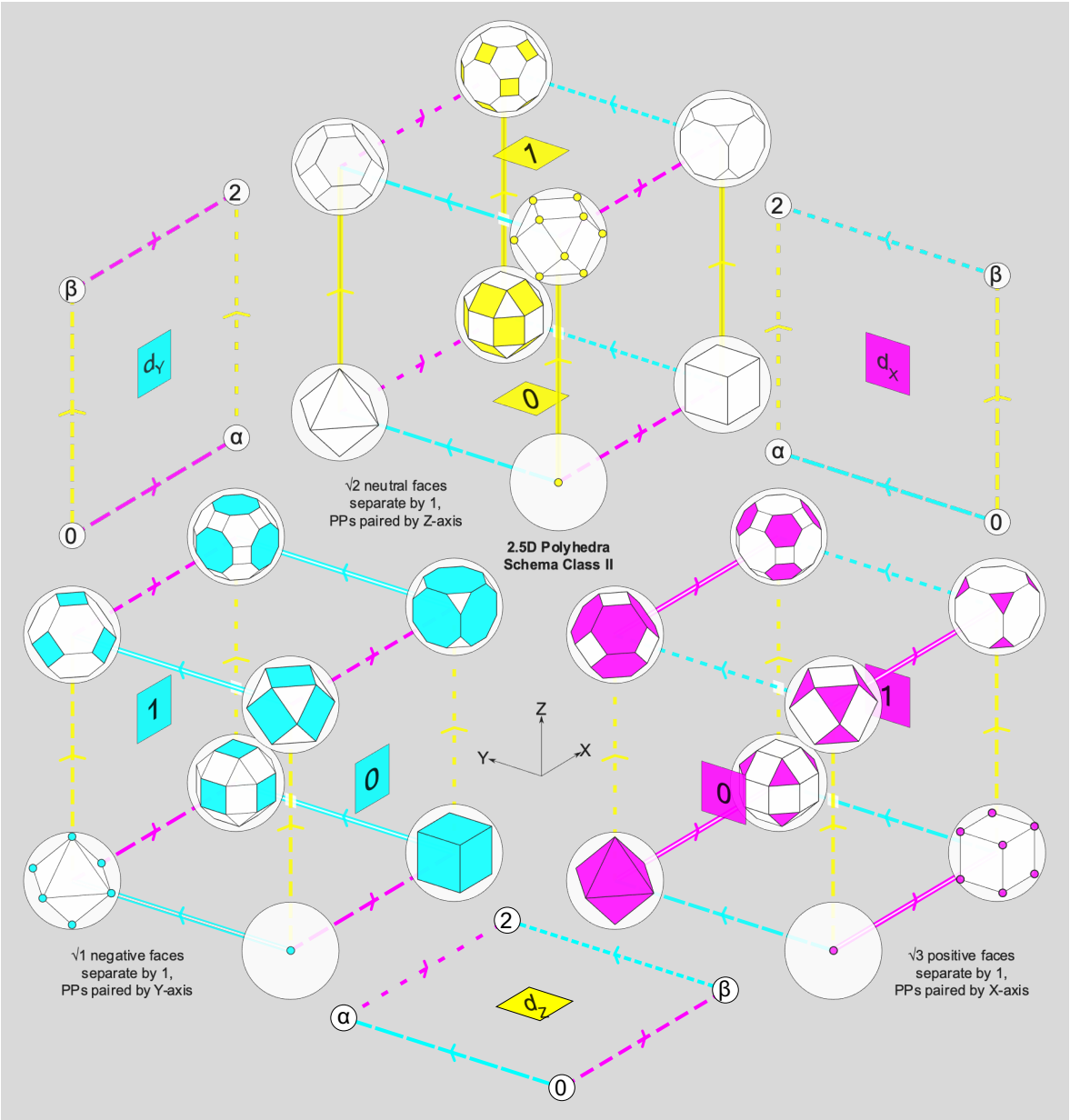

Fig. 13: The simultaneous various facial evolutions. Double lines of cyan, yellow, magenta denote the separation of faces for the respective −ve Y, ntrl Z, +ve X (lower left, top, lower right) axes. Single lines of varied dash of such coloring denote the simultaneous evolution of faces of two paired (0→α) & (α→2), and (0→β) & (β→2), with *PP* faces cyan, yellow, magenta, respectively. In each schematic cube, the 4 −ve, ntrl, or +ve parallel lines denoting the evolution of faces correspond to the bundles of edges of the three zones of the cubic zonahedron. The double line zonal bundle separates the two faces of the schematic cube as enantiomorph of the rhombic schema, the polytopes of one face for d=0 where faces adjoin (sharing a common vertex or edge), while those of the opposing face for d=1 where the faces are adjacent (separated by unit distance). The −ve, ntrl, +ve rhombs for the Y, Z, X axes are abstracted at top left, bottom, top right, respectively. All 3 cubic schema apply simultaneously; the −ve and +ve cubic schema are bilaterally symmetric, the transformations of the schema applying to the relationships (edges), not the *PP*s. All five classes demonstrate the same morphology, allowing for the dimensional difference between the polyhedra and polygonal tessellations (Classes I–III *cf.* IV & V).

6. CONCLUSION

Earlier apprehension [11, 12] suggested that the elegance of the regular and semiregular polyhedra and tessellations was surely matched by their order, and has inspired subsequent research.

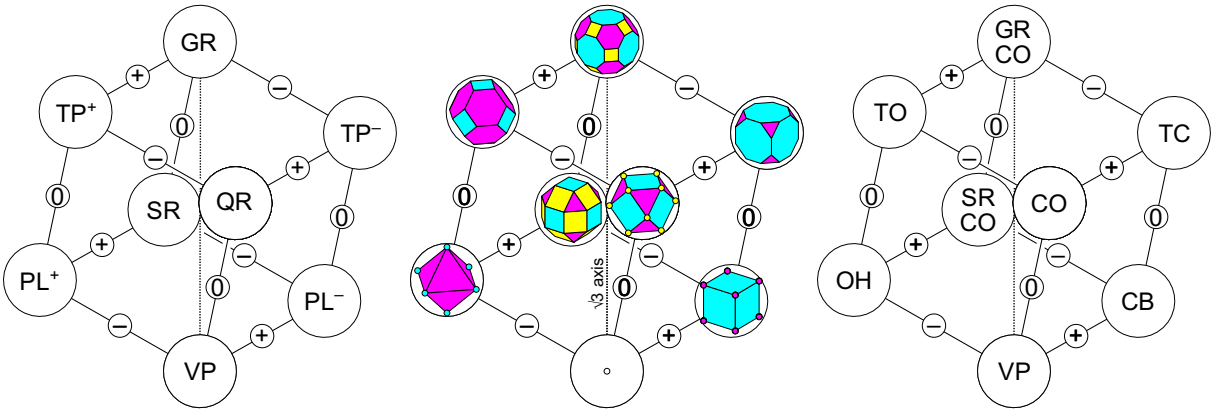

Fig. 14: Separation of faces by −ve/ntrl/+ve gender. Each transition $PP_0 \rightarrow PP_1$ is characterized by a separation of neighboring faces from adjoining (d=0) to adjacent (d=1), in 3 X,Y,Z zones. Left to right: Generic, Class II polytopes, & IDs. *PP*s evolve (devolve) upwards (downwards) $VP \rightarrow GR$ ($GR \rightarrow VP$).

Inspection of this schema (Fig. 14) shows that any *PP* transition $PP_0 \rightarrow PP_1$ is characterized by a separation of neighboring faces from adjoining (d=0) to adjacent (d=1), in one of the 3 X, Y, or Z zones.

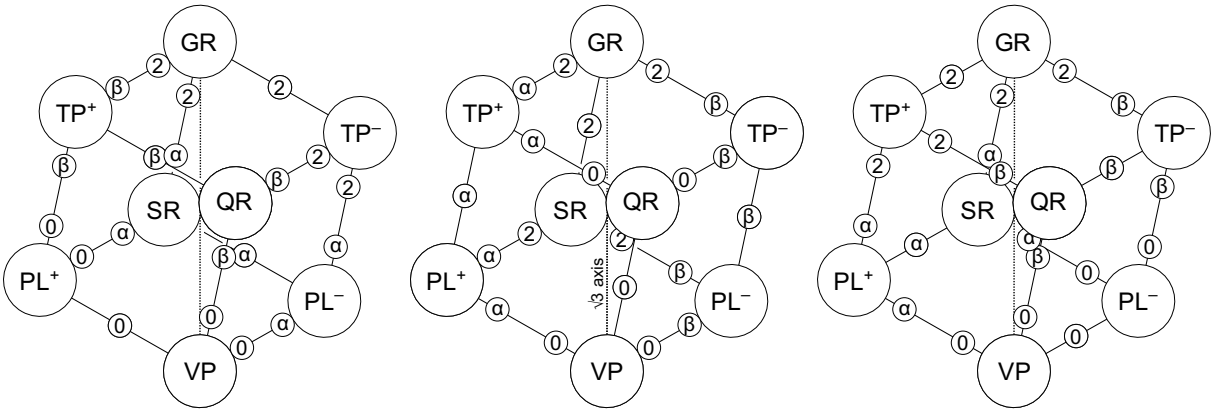

Fig. 15: Simultaneous transformation of faces by (0→α|β→2) evolution. As faces of one −ve/ntrl/+ve gender separate, faces of the remaining two genders transform, in pairs of transitions of ***PP***s of each zone. Quartiles show facial evolutionary stage, with zones in (0→α, β→2) or (0→β, α→2) pairs. Mid-points conserve facial separation, each zone with 1 (0, α, β, 2) face. Left to right: −ve; ntrl; +ve faces.

Figure 15 demonstrates that for each case of −ve, ntrl, and +ve faces, as one zone of the cubic schema represents the separation of −ve, ntrl, or +ve faces, respectively, one of the other two zones represents two pairs of parallel 0→α and β→2 transitions, while the other zone represents two pairs of parallel 0→β and α→2 transitions. Figure 16 shows that for each case of −ve, ntrl, and +ve faces, the X, Y, or Z axial zone of separation of faces representing 0→0, α→α, β→β, and 2→2 of the cubic schema of d=0 and d=1, respectively, separates two corresponding rhombic schema of d=0 and d=1, respectively, as previously shown in Fig. 10.

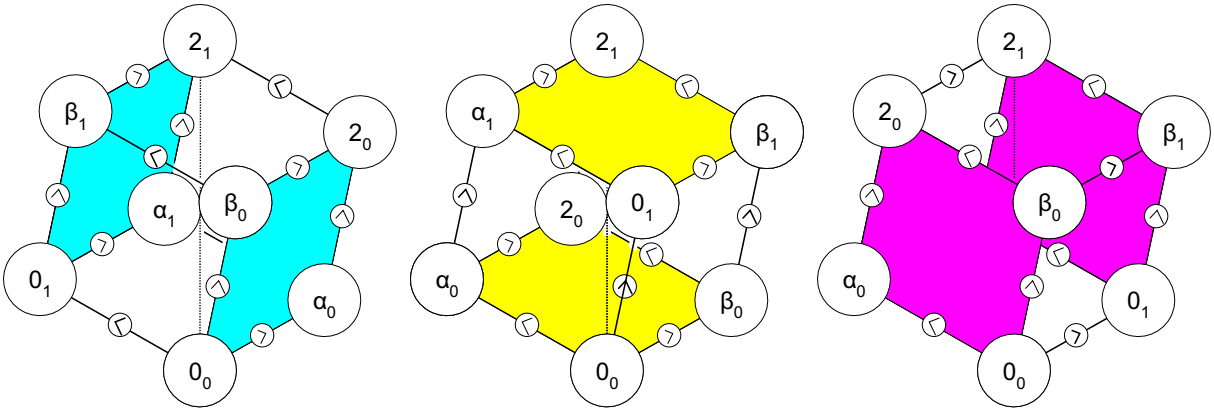

Fig. 16. Y, Z, & X zone separation of d=0 & d=1 rhombic schema of −ve, ntrl, +ve faces (L to R).

Thus, the separation of faces appears fundamental to the progression of PPs represented by the edges of the cubic schema. That separation of faces for one gender is complemented by the simultaneous morphing of the faces of the other two genders according to either of two opposite edges of the rhombic schema of (0→α and β→2), or (0→β and α→2), respectively.

This elegant morphology appears to characterize the order of the regular and semi-regular polyhedra and tessellations. Consequent upon the assumption of a null polytope in each of the five symmetry classes; the assumption of degenerate 0D and 1D facial polytopes of certain vertices and edges by gender; the cubic schema of PPs; its rotation to the vertical $VP \rightarrow GR$ √3 axis; the rhombic schema (in both enantiomorphs) of null 0, regular α or quasi-regular β, and $2f$ faces; the notion of limited 3-fold symmetry to the order; the fundamental separation of faces d=0 to d=1; and accommodation of the transitional form of the snub enantiomorphs of each class at the center of the cubic schema, at the mid-point of the $SRQR$—QR jitterbug and main VP—GR axes, the order of the polyhedra and tessellations is herein adequately described.

This work might find application to diverse fields of polyhedral geometry, crystallography, chemistry (phase transitions, bi-polymers, smart polymers, catalysts), artificial bone matrix integrating variable flexibility, biomedicine (triggered deployment of dosage of drug from nanocages), smart material, wearable (conformable) electronics, space structures (dynamic structures, deployable antennae in Space), nanostructures, perhaps quantum mechanics and field theory, and potentially the nature of space itself. Future research is intended to refine the order of the all-space-filling periodic arrays of 2D & 3D PTs in the light of this cubic schema.

Historically, the regular (and semi-regular) polyhedra as independent entities have been recognized as perfect (and semi-perfect) forms. However, while such formal perfection should at the very least be matched in their overall structure and morphology, I am unaware of any adequate order having previously been advanced. This paper redresses that shortfall with reference to the separation of one set of +ve, ntrl, or −ve faces characterizing the zonahedral progression of PP_1 to PP_2 on the rotated 2.5D cubic schema, while the other two sets of faces evolve according to the rhombic schema. It has been a privilege to glimpse such perfection.

***

7. REFERENCES

1. K. Critchlow, Order in Space. Thames and Hudson, London, 1969.
2. B. Grünbaum and G. C. Shephard, Tilings and Patterns. W. H. Freeman, New York, 1987.
3. R. C. Meurant, A Novel 2.5D Schema of the Regular and Semi-regular Polytopes and their Sequences, with Analysis by Polytope and Surface Elements. Information Journal, International Information Institute, Vol.24, No.2, June 2021, pp.51–64. PDF 68.
4. R. C. Meurant, A New 2.5D Schema of the Regular & Semi-regular Polyhedra and Tilings: Classes II and IV. *Information*, L. Li, R. Ashino, & C.-C. Hung (eds.), Proceedings of The Tenth International Conference on Information, Tokyo/Zoom, Mar. 6–7, 2021, 29–34. PDF 67.
5. R. C. Meurant, Towards a New Order of the Polyhedral Honeycombs: Part III: The Developed Metaorder, Form and Counterform. *Information*, Vol.22, No.1, Jan. 2019, 23–45. PDF 66.
6. R. C. Meurant, Form and Counterform in the Periodic Polyhedral Honeycombs. Information 2018: L. Li et al. (eds.), Proc. of The 9th Int. Conf. on Information, Tokyo, Dec. 7–9, 2018, 51–56. PDF 65.
7. R. C. Meurant, Expansion Sequences and their Clusters of the All Space-filling Periodic Polyhedral Honeycombs. *Information*, Vol.20, No.10(A), Oct. 2017, 7345–7362. PDF 64.
8. R. C. Meurant, Sequences of the All Space-filling Periodic Polyhedral Honeycombs. Information 2017. L. Li et al. (eds.), Proceedings of The Eighth International Conference on Information, Tokyo, May 17–18, 2017, 151–154. PDF 63.
9. R. C. Meurant, Towards a Meta-Order of the All-Space-Filling Polyhedral Honeycombs through the Mating of Primary Polyhedra. *Information*, Vol.19, No. 6(B), June 2016, 2111–2124. PDF 62.
10. R. C. Meurant, Towards a New Order of the Polyhedral Honeycombs: Part II: Who Dances with Whom? Information 2015: L. Li and T.-W. Kuo (eds.), Proceedings of The Seventh International Conference on Information, Taipei, Nov. 25–28, 2015, 369–373. PDF 61.
11. R. C. Meurant, A New Order in Space – Aspects of a Three-fold Ordering of the Fundamental Symmetries of Empirical Space, as evidenced in the Platonic and Archimedean Polyhedra – Together with a Two-fold Extension of the Order to include the Regular and Semi-regular Tilings of the Planar Surface. *Int. J. of Space Structures*, Vol.6 No.1, Univ. of Surrey, Essex, 1991, 11–32. PDF 06.
12. R. C. Meurant, The Aesthetics of the Sacred: A Harmonic Geometry of Consciousness and Philosophy of Sacred Architecture (3rd ed.), The Opoutere Press 1989 ISBN 0-908809-02-6. (PhD thesis, Univ. of Auckland, 1984). Available from the author, see http://www.rmeurant.com/its/books.html
13. R. C. Meurant, The Myth of Perfection of the Platonic Solids. People and Physical Environment Research PAPER Conference on Myth Architecture History Writing, University of Auckland, New Zealand, July 1991. PDF 07.

Supplementary Information: References [3−11, 13] as PDFs (68−61, 06, 07), and PDF 69 of this paper, in color or greyscale, are available at http://www.rmeurant.com/its/papers/polygon-1.html

Nomenclature: non-dimensional: –ve, negative; ntrl, neutral; +ve, positive; f, frequency (of F); GR, great rhombic; $L0{-}L2$, level (0, 1= α & β, 2) of rhombic schema; P, pole or polar; $S1-4$, strata (1–4) of rotated cubic schema; Snb, snub; SR, small rhombic; $Trnc$, truncated. ● zero-dimensional: V^0, neutral vertex (NV); V, vertex (but can be 1 or 2D 'F'); VP, verticial polytope hence VP_{I-V}. ● one-dimensional: d, distance of proximal Fs (0 or 1); E, edge (EG) but here can be 2D 'F'; E^0, neutral edge (NE) but here 2D 2-gon 'F'. ● two-dimensional: DD, dodecagon (12-gon); HX, hexagon or hexagonal array; OG, octagon; PR, polar polygon; RH, rotated hexagon; RP, 'rotated' polar polygon (trunc.); RS, 'rotated' (trunc.) square; RT, 'rotated' (trunc.) triangle; RX, 'rotated' (trunc.) hexagon; SQ, square; SQ^0, neutral square (NS); $SQ{:}SQ$, square–square array; TP, truncated polar polygon ($2f$); TR, triangle or triangular array; $TR{:}HX$, tri-hex array; $TrncHX$, truncated hexagonal array; $TrncTR$, truncated triagonal array; ZG, zonagon. ● three-dimensional: CB, cube; CO, cuboctahedron; DC, dodecahedron; $GRCO$, great rhombic cuboctahedron; IC, icosahedron; $IC{:}DC$, icosidodecahedron; OH, octahedron; $OH{:}CB$, octahexahedron (= CO); $SnbCO$, snub cuboctahedron; $SRCO$, small rhombic cuboctahedron; TC, truncated cube; TD, truncated dodecahedron; TH, tetrahedron; $TH{:}TH$, tetra-tetrahedron (Class I colored OH); TI, truncated icosahedron; TO, truncated octahedron; TP, truncated polar polytope; TT, truncated tetrahedron; ZH, zonahedron. ● multi-dimensional: F, face = facial PT (in this paper, 0D, 1D, or 2D); α, regular facial polytope; β, quasiregular facial polytope; $GRQR$, great rhombic quasiregular; PL, polar polytope; PP, primary polytope; PT, polytope; QR, quasiregular; $SnbQR$, snub quasiregular; $SRQR$, small rhombic quasiregular. ■

Robert C. Meurant □ B.Arch (Hons) (1978), and PhD in Architecture (1984), University of Auckland, New Zealand □ MA in Applied Linguistics (2007), University of New England, Australia □ Director Emeritus, Institute of Traditional Studies, founded 1984 □ Taught in universities in New Zealand, the United States, and Korea □ Published 6 books, 70 papers, presented papers in New Zealand, the U.S., the U.K., Japan, and Korea □ For many years, a director of the Science & Engineering Research Support Society (SERSC), Korea □ Research interests: sacred and traditional geometry, art, and architecture; the traditional philosophy of art; number and form; the polyhedra; structural morphology and geometry; deployable Space habitation and large-scale structures in microgravity, nanoarchitecture, applied linguistics ■